

Stars and brown dwarfs in the σ Orionis cluster

IV. IDS/INT and OSIRIS/GTC spectroscopy and *Gaia* DR2 astrometry[★]

J. A. Caballero¹, A. de Burgos^{2,1}, F. J. Alonso-Floriano^{3,4}, A. Cabrera-Lavers^{5,6,7},
D. García-Álvarez^{5,6,7}, and D. Montes⁴

¹ Centro de Astrobiología (CSIC-INTA), ESAC, camino bajo del castillo s/n, 28691 Villanueva de la Cañada, Madrid, Spain
e-mail: caballero@cab.inta-csic.es

² Isaac Newton Group of Telescopes, apartado de correos 321, 38700 Santa Cruz de La Palma, La Palma, Spain

³ Leiden Observatory, Leiden University, PO Box 9513, 2300 Leiden, The Netherlands

⁴ Departamento de Física de la Tierra y Astrofísica & IPARCOS-UCM (Instituto de Física de Partículas y del Cosmos de la UCM),
Facultad de Ciencias Físicas, Universidad Complutense de Madrid, 28040 Madrid, Spain

⁵ Instituto de Astrofísica de Canarias, Avenida Vía Láctea, 38205 La Laguna, Tenerife, Spain

⁶ Grantecan S. A., Centro de Astrofísica de La Palma, Cuesta de San José, 38712 Breña Baja, La Palma, Spain

⁷ Departamento de Astrofísica, Universidad de La Laguna, 38205 La Laguna, Tenerife, Spain

Received 30 May 2019 / Accepted 7 August 2019

ABSTRACT

Context. Only a few open clusters are as important for the study of stellar and substellar objects, and their formation and evolution, as the young σ Orionis cluster. However, a complete spectroscopic characterisation of its whole stellar population is still missing.

Aims. We filled most of that gap with a large spectroscopic and astrometric survey of targets towards σ Orionis. Eventually, it will be one of the open clusters with the lowest proportion of interlopers and the largest proportion of confirmed cluster members with known uncontroversial youth features.

Methods. We acquired 317 low-resolution optical spectra with the Intermediate Dispersion Spectrograph (IDS) at the 2.5 m *Isaac Newton* Telescope (INT) and the Optical System for Imaging and low Resolution Integrated Spectroscopy (OSIRIS) at the 10.4 m Gran Telescopio Canarias (GTC). We measured equivalent widths of Li I, H α , and other key lines from these spectra, and determined spectral types. We complemented this information with *Gaia* DR2 astrometric data and other features of youth (mid-infrared excess, X-ray emission) compiled with Virtual Observatory tools and from the literature.

Results. Of the 168 observed targets, we determined for the first time spectral types of 39 stars and equivalent widths of Li I and H α of 34 and 12 stars, respectively. We identified 11 close ($\rho \lesssim 3$ arcsec) binaries resolved by *Gaia*, of which three are new, 14 strong accretors, of which four are new and another four have H α emission shifted by over 120 km s⁻¹, two juvenile star candidates in the sparse population of the Ori OB1b association, and one spectroscopic binary candidate. Remarkably, we found 51 non-cluster-members, 35 of which were previously considered as σ Orionis members and taken into account in high-impact works on, for example, disc frequency and initial mass function.

Key words. open clusters and associations: individual: σ Orionis – stars: early-type – stars: solar-type – stars: late-type – stars: emission-line, Be – stars: pre-main sequence

1. Introduction

There are a few nearby young clusters, such as the Pleiades and the Hyades, whose stellar (and substellar) populations have been investigated in detail for decades, which translates into hundreds of known Pleiads and Hyads (Johnson & Mitchell 1958; Herbig 1962; Chaffee et al. 1971; Vandenberg & Bridges 1984; Boesgaard & Tripicco 1986; Soderblom et al. 1993; Perryman et al. 1998; Stauffer et al. 1998; Bouvier et al. 2018; Martín et al. 2018, to cite just a few examples). As a result, these clusters are cornerstones for the study of the formation and evolution of stars.

The very young σ Orionis open cluster ($\tau \sim 3$ Ma, $d \sim 388$ pc), near the Horsehead nebula in the Ori OB1b association, is one of the most attractive and most visited regions for night-sky observers, both professional and amateur. This

cluster was discovered by Garrison (1967), re-discovered by Wolk (1996), introduced to a new era by Béjar et al. (1999) and Zapatero Osorio et al. (2000), and finally reviewed by Walter et al. (2008) and Caballero (2008a). At that stage, σ Orionis became one of the best-studied young open clusters together with the Pleiades and the Hyades, and at the same level of importance as other very young open clusters and star-forming regions, such as the Trapezium, Taurus-Auriga, or ρ Ophiuchi, which are affected by (spatially variable) extinction. A major event in the history of σ Orionis studies was the computation of a continuous mass function from about 20 M_{\odot} to only about 0.005 M_{\odot} by Peña Ramírez et al. (2012). For that, these latter authors complemented their very deep VISTA survey with the Mayrit catalogue of σ Orionis stars and brown dwarfs (Caballero 2008a), which remains the most comprehensive database of cluster members. This catalogue was the first item of the paper series “Stars and brown dwarfs in the σ Orionis cluster”, which was continued by Caballero (2010a), who conducted a pre-*Gaia* proper-motion analysis,

[★] Full Tables A.1–A.5 are only available at the CDS via anonymous ftp to cdsarc.u-strasbg.fr (130.79.128.5) or via <http://cdsarc.u-strasbg.fr/viz-bin/cat/J/A+A/629/A114>

Table 1. Observations of standard stars for the OSIRIS spectral type classification.

Name	GJ	α (J2000)	δ (J2000)	Spectral type	Ref.	Date of observation	t_{exp} [s]
HD 88230	380	10 11 22.14	+49 27 15.3	K7 V	Kir91	20 Dec. 2012	2×0.5
BD+33 1505	270	07 19 31.27	+32 49 48.3	M0.0 V	AF15	09 Dec. 2012	2×60
BD+02 2098	328	08 55 07.62	+01 32 47.4	M0.0 V	Lép13	20 Dec. 2012	2×60
HD 36395	205	05 31 27.40	-03 40 38.0	M1.5 V	AF15	09 Dec. 2012	2×90
HD 209290	846	22 02 10.26	+01 24 00.6	M0.5 V	AF15	09 Dec. 2012	1×120
LP 379-51 ^(a)	3790	13 31 50.57	+23 23 20.3	M2.5 V	Lep13	16 Mar. 2012	2×30
Ross 1022 ^(a)	3795	13 38 37.05	+25 49 49.7	M3.0 V	Lep13	16 Mar. 2012	3×30
FN Vir ^(a)	493.1	13 00 33.51	+05 41 08.2	M4.5 V	Dav15	16 Mar 2012	2×60
LP 799-7 ^(a)	3820	13 59 10.46	-19 50 03.5	M4.5 V	Ria06	16 Mar. 2012	3×60
LP 380-6 ^(a)	1179A	13 48 13.41	+23 36 48.8	M5.0 V	New14	16 Mar. 2012	2×90
LP 731-58 ^(a)	3622	10 48 12.58	-11 20 08.2	M6.5 V	AF15	22 Mar. 2012	2×60

Notes. ^(a)Targets previously observed by Caballero et al. (2012).

References. Kir91: Kirkpatrick et al. (1991); Ria06: Riaz et al. (2006); Lep13: Lépine et al. (2013); New14: Newton et al. (2014); Dav15: Davison et al. (2015); AF15: Alonso-Floriano et al. (2015).

and by Caballero et al. (2012), who reviewed the most relevant publications on the cluster between 2008 and 2012, published a number of low-resolution optical spectra of member stars and brown dwarfs that lacked previous spectroscopy, and updated the Mayrit catalogue. However, the results presented by Caballero et al. (2012) were superseded by the spectroscopic census of Hernández et al. (2014), which constitutes the largest homogeneous spectroscopic data set of the σ Orionis cluster to date.

In the last lustrum, the Mayrit catalogue has been used for searching for pulsations and photometric variability in substellar objects (Cody & Hillenbrand 2014; Elliott et al. 2017), extending spectroscopic surveys to the lowest masses and the largest separations to the cluster centre (Koenig et al. 2015; Zapatero Osorio et al. 2017; Cottle et al. 2018), characterising discs with theoretical models and ALMA and *Spitzer* observations (Álvarez-Meraz et al. 2017; Ansdell et al. 2017; Winter et al. 2018; Pérez-Blanco et al. 2018), identifying large-scale Herbig-Haro jets driven by proto-brown dwarfs (Riaz et al. 2017, 2019), and carefully analysing the massive multiple stellar system that gives the name to the cluster (Simón-Díaz et al. 2015; Schaefer et al. 2016), not counting the studies performed by the first author and his colleagues on multiplicity (Caballero 2014; Caballero et al. 2016, 2018) and parallaxes and proper motions (Caballero 2017, 2018).

In spite of all these studies, there are still a number of photometric cluster member candidates in both stellar and substellar regimes that lack membership confirmation. Furthermore, beyond the cluster core and at angular separations greater than 20 arcmin from the cluster centre at the eponymous σ Ori Trapezium-like system (Caballero 2008b), the contamination by distinct populations of young stars in the Ori OB1b association continues to increase. Neighbouring populations have been reported towards the younger Horsehead and Flame nebulae to the east and the older ϵ Orionis cluster to the north and west, but there are also hints of a sparse population of 5–30 Ma-old stars in the cluster foreground. Such distinct populations may have different photometric, kinematic, and spectroscopic properties from those of σ Orionis (Jeffries et al. 2006; Sacco et al. 2007, 2008; Caballero & Solano 2008; Maxted et al. 2008; Hernández et al. 2014; Kounkel et al. 2018; Riaz et al. 2019), but disentangling them in the cluster halo ($\rho \approx 20$ –30 arcmin) requires a careful analysis. Here we use low-resolution optical spectroscopy,

complemented with *Gaia* astrometry, for studying the σ Orionis membership of a large sample of stars and brown dwarfs.

2. Data and analysis

2.1. Sample

We obtained 317 low-resolution, long-slit optical spectra of 168 different sources comprising mostly high-to-low-mass stars selected from different surveys. Our sample includes OB, Herbig Ae/Be, T Tauri, variable, and binary stars, as well as brown dwarfs, in σ Orionis, but also young stars in neighbouring star-forming regions, fore- and background stars, and even one active galaxy. Most of them have youth features such as X-ray emission, mid-infrared excess, strong broad H α emission, and Li I absorption, and have been identified as genuine σ Orionis cluster members using different techniques (e.g. Walter et al. 2008; Caballero 2008a, 2017; Hernández et al. 2014 – see below), while others are new member candidates or photometric candidates. As detailed in Sect. 2.2.1, 142 of those targets were observed with the *Isaac Newton* Telescope (INT) and 47 with the Gran Telescopio Canarias (GTC). For comparison purposes, 21 of them were observed with both telescopes. With GTC, we also observed 11 nearby standard stars with spectral types between K7 V and M6.5 V, which are listed in Table 1. The GTC spectra corresponding to 11 sources towards σ Orionis and six standard stars were previously published by Caballero et al. (2012).

2.2. Spectroscopy

2.2.1. Observations and reduction

The IDS at the INT. Observations at intermediate and low resolution were carried out using the Intermediate Dispersion Spectrograph (IDS) at the 2.5 m INT located at the Observatorio del Roque de los Muchachos in La Palma, Canary Islands, Spain. The IDS is a long-slit spectrograph attached at the INT Cassegrain focus equipped with a 235 mm focal length camera with two different possible $4k \times 2k$ CCD detectors. For this work we used the EEV10 CCD. This latter is a blue-sensitive ($>50\%$ efficiency from 400 to 700 nm) CCD that provides a spatial scale of $0.40 \text{ arcsec pixel}^{-1}$ and an unvignetted

Table 2. Date of observations and instrument configurations.

Date of observations	Instrument	Grism	Slit width [arcsec]	Resolution	$\Delta\lambda$ [Å]	λ_{central} [Å]
22–27 Feb. 2007	IDS	R1200Y	1.515	1300	5750–6850	6300
28 Feb. 2007	IDS	R150V	1.515	460	3700–7500	5500
04–22 Mar. 2012	OSIRIS	R1000B	1.23	660	3700–7800	5750
Nov.–Dec. 2012, Jan. 2013	OSIRIS	R1000B	1.23	660	3700–7800	5750

3.3 arcmin (500 pixels) slit length. All observations with IDS were performed in parallactic angle on six consecutive nights from 22 to 28 February 2007. We used two different gratings: R1200Y, which provides >60% efficiency at 6000 Å and a spectral resolution of ~ 1300 , on the first five nights, and R150V, which provides a similar efficiency with a wider wavelength range but three times lower resolution, on the last night. Our instrument configuration is in Table 2.

The aim of the telescope proposal was to obtain optical spectroscopy of the 100 brightest young stars in σ Orionis, as well as of the maximum number possible of bright interloper stars towards the cluster. We list the names, equatorial coordinates, and main observing parameters of the 142 observed targets in Table A.1. We provide both the Mayrit identifier (Caballero 2008a) and the alternative (discovery) name for σ Orionis members. We took equatorial coordinates from *Gaia* DR2 (Gaia Collaboration 2016, 2018) in all cases except for a few particular ones, indicated in the table. We tabulate coordinates of the primary in close binary systems resolved by *Gaia* (Sect. 2.3). Six stars were observed with the two IDS gratings. Several stars were also observed a few times for improving the spectral signal-to-noise ratio but avoiding saturation (e.g. σ Ori AB), for daily monitoring (e.g. σ Ori E), or for minimising contamination using angles different from parallactic angle (e.g. 2MASS J05384652–0235479 = [BHM2009] SigOri-MAD-23, halfway between σ Ori AB and E). The weather during the observations was good in general, but with a variable seeing from 0.8 to 2.0 arcsec.

Data reduction was carried out using standard tasks within the IRAF software environment. The reduction of the 193 IDS spectra included bias and flat-field correction, removal of sky background, optimised aperture extraction, wavelength calibration using Cu–Ar and Cu–Ne arc lamps, instrumental response correction (calibrated with flux standard stars observed on the same nights for another programme), and hot-pixel and cosmic-ray removal. We checked the logbooks of the IDS observations for mistakes in target names, as well as for relevant remarks regarding signal-to-noise ratios or observed features. For stars with multiple observations and low signal-to-noise-ratio spectra (and the same grism), we combined the individual spectra for a higher signal. The spectra of two stars, 2MASS J05384652–0235479 and 2MASS J05381494–0219532, were of poor quality because of contamination from nearby sources and were discarded from the following analysis. The spectra of 18 normalised, fully reduced IDS spectra from O9.5+V to M6 are shown in Fig. A.1.

The OSIRIS at the GTC. Observations were also carried out using the Optical System for Imaging and low Resolution Integrated Spectroscopy (OSIRIS) tunable imager and spectrograph (Cepa et al. 2000; Cepa 2010) at the 10.4 m GTC located at the Observatorio Roque de los Muchachos in La Palma, Canary Islands, Spain. OSIRIS has a mosaic of two $4k \times 2k$ e2v Marconi CCD44-82-BI detectors, which provides an

unvignetted field of view of 7.8×7.8 arcmin² with a spatial scale of 0.127 arcsec pixel⁻¹. To increase the signal-to-noise ratio, we selected the standard operation mode of the instrument, which implements a 2×2 binning mode with a readout speed of 100 kHz. All observations were carried out using the R1000B grism, which provides a peak efficiency of 65% at 5455 Å and covers the optical wavelength up to 7800 Å. Again, our instrument configuration is in Table 2.

The observations with OSIRIS were performed in service mode on different nights in March, November, and December 2012, and January 2013, through “D-band” filler programmes¹ (Table A.2). Observations before 01 April 2012 were presented by Caballero et al. (2012). We list the names, equatorial coordinates, and main observing parameters of the 47 observed targets in Table A.2. As for IDS, we provide both the Mayrit identifiers and the alternative (discovery) name for the cluster members. We took coordinates from *Gaia* DR2 except for one source, indicated in the table. The aim of this filler programme was to obtain, within the GTC nightly operation schedule, high-quality low-resolution spectra of variable M stars with no previous spectroscopic characterisation and spectral type determination that are relatively bright for a 10 m-class telescope (with magnitudes of up to $V \sim 19$ mag) but under poor weather conditions. However, the weather conditions were not very bad in general except for a few nights with dust and poor seeing. Most of the targets were observed at an airmass ≤ 1.6 .

Data reduction was carried out using standard tasks within the IRAF software environment as in Caballero et al. (2012). All the 124 spectra of 47 sources towards Orion and 11 standard stars were bias-subtracted, corrected from flat-field using lamp flats from the GTC instrument calibration module, and were calibrated in wavelength using Xe, Ne, and Hg–Ar arc lamps. The reduction was followed by a sky-background subtraction and a one-dimension spectrum extraction, which were done taking into account the seeing conditions and exposure times. Finally, we applied a hot-pixel and cosmic-ray removal. The corresponding instrument-response correction was exactly the same as in Caballero et al. (2012). As for IDS, we combined the individual spectra of stars with multiple observations and with low signal-to-noise ratio (and the same grism). We discarded from the following analysis the source 2E 1456 (UCM0535–0246), a Seyfert 1 galaxy at $z \sim 0.1$ previously considered to be a reddened low-mass σ Orionis member (Caballero et al. 2012). The spectra of five normalised, fully reduced OSIRIS spectra onto the spectral grid of the 11 standard stars are shown in Fig. A.2.

¹ D-band proposals (or fillers) require very relaxed observing conditions and cover a wide range of coordinates so that they can be carried out at essentially any moment during the semester. Observations in this band are only executed if the observing conditions do not permit observations of proposals in A, B, or C bands (<http://www.gtc.iac.es/observing/>).

2.2.2. Equivalent widths

After discarding the two stars with poor-quality spectra and the galaxy, we kept 165 stars and brown dwarfs for the analysis. In the spectra of all of these objects, we measured equivalent widths (EWs) with errors of key spectral line targets using the IRAF `sp1ot` task and the “equivalent width” function (conversely, we measured pseudo-EWs with respect to the pseudo-continuum in the K and M star spectra). For both IDS and OSIRIS spectra, we measured EWs of the Balmer lines $H\alpha$ λ 6562.80 Å, $H\beta$ λ 4861.33 Å, and the helium triplet He I D₃ λ 5875.67 Å in emission, and the lithium line Li I λ 6707.80 Å in absorption. For OSIRIS we also measured the calcium doublet Ca H&K λ 3933.66,3968.47 Å and the Balmer line H γ λ 4340.47 Å, which were present in most of the spectra, but also the Balmer H δ , H ζ , H η , H10, H11, H12 lines, the Mg I b triplet, the Na I D₁₋₂ doublet (measured as a singlet because of the low resolution) and the He I line at λ 6678.15 Å when measurable. Measured EWs of H β , He I D₃, H α , Li I (IDS and OSIRIS), Ca K, and Ca H (OSIRIS only) are shown in Tables A.3 and A.4.

2.2.3. Spectral types

For each target, we determined spectral types using the spectrum with the highest signal-to-noise ratio. For the targets observed at the INT with both R1200Y and R150V grisms we used only R1200Y. Depending on the instrument and stellar effective temperature, we followed three different strategies for determining the spectral type of all the stars.

MILES. We derived spectral types of the 140 analysable stars observed with IDS by comparing their spectra with synthetic ones generated with the MILES “Spectra by Stellar Parameters” webtool² (Sánchez-Blázquez et al. 2006; Vazdekis et al. 2010; Falcón-Barroso et al. 2011). This tool allows the generation of synthetic stellar spectra of stars from 36 000 K down to 2750 K, which approximately correspond to O9 to M6 main sequence spectral types. The MILES spectra fully cover the range of spectral types in our sample and the wavelengths of most IDS spectra with a comparable spectral resolution (MILES: 0.90 Å pixel⁻¹; R1200Y IDS: 0.48 Å pixel⁻¹). However, MILES oversamples the spectra taken with the R150V grism, which has a dispersion of 3.66 Å pixel⁻¹. For generating our own library of synthetic spectra, we used MILES with solar metallicities and surface gravities varying with effective temperature as described by Popper (1980). For the relation between temperatures and spectral types we used the relationships of Pecaut & Mamajek (2013) for K and M spectral types and those of Cox (2001) for earlier types. To perform the spectral type identification, first we classed the 140 spectra into 14 groups, sorted the spectra by approximate effective temperature within each group, and assigned a real (non-synthetic) MILES spectrum to each group. This grouping helped us to narrow down the interval of effective temperatures and surface gravities of each individual star, and to determine spectral types with a precision of about one subtype via a χ^2 minimisation as in Alonso-Floriano et al. (2015). The results are listed under “SpT MILES” in Table A.3.

Standard stars. We derived spectral types of the 46 stars and brown dwarfs observed with OSIRIS towards σ Orionis using standard stars from K7 to M6.5 (Table 1), with a spectral typing precision of one subtype in this range. We assigned spectral types by fitting by eye the problem star to our grid

² <http://www.iac.es/proyecto/miles/pages/webtools.php>

of standard stars, which were observed with exactly the same instrument configuration (Fig. A.1). We took care to properly fit the (pseudo-)continuum and the strongest lines and bands in absorption, for which accurate wavelengths were taken from the “The Atomic Line List” webtool³. Unexpectedly, several stars had spectral types earlier than K7. A χ^2 fitting as with MILES did not improve our visual determination. The results are listed under “SpT Standards” in Table A.4.

PyHammer. In addition to the previous strategies, we also used the “PyHammer” Python Spectral Typing Suite⁴ from Covey et al. (2007). PyHammer uses its own empirical templates of spectral types and metallicities to estimate the spectral type of a star by measuring prominent line indices and performing a weighted least-squares minimisation. It covers spectral types from O5 to L3 and metallicities from -2.0 dex to $+1.0$ dex. We applied the PyHammer algorithm to all our spectra from both IDS and OSIRIS. According to Covey et al. (2007), the accuracy provided by The Hammer, the basis on which PyHammer was built, is of around two subtypes. Having not investigated the differences between automatic and visual classifications of PyHammer, we assumed that the results are similar to those with The Hammer and OSIRIS/GTC as reported by Metodieva et al. (2015), who pointed out the improved accuracy of the tool for late M dwarfs. The resulting spectral types are listed in Tables A.3 and A.4 under “SpT PyHammer”.

Adopted spectral type. We report the finally adopted spectral type in Table A.5. In particular, we followed these criteria. We used the standard stars strategy for stars with spectral types K7–M6.5 observed with OSIRIS. For stars earlier than K7 observed with OSIRIS we used literature information (Mayrit 783254, 931117, 1042077, and [HHM2007] 648 from Hernández et al. 2014), PyHammer (Mayrit 1223121), or classical visual inspection of spectral features (Haro 5-17 and [HHM2007] 829). We used MILES for stars later than B0 observed with IDS (including those observed with OSIRIS). Finally, we used literature information for stars earlier than B0 observed with IDS (σ Ori AB itself; Simón-Díaz et al. 2015).

Of the 165 analysed stars, we present spectral types for the first time for 39 of them, and improve previous determinations in a few cases. In Fig. 1, we compare our spectral types to those of the literature. For example, there are half a dozen mid-K non-cluster-members that were classified as mid-G stars by Hernández et al. (2014). Figure 1 shows another two extreme outlier examples. Apart from these differences, the agreement with previous spectral determinations is generally within one or two subtype uncertainties.

2.3. Gaia DR2

At the moment of observation, equatorial coordinates were taken from the Two-Micron All-Sky Survey (2MASS; Skrutskie et al. 2006). However, we tabulate here the latest Gaia DR2 coordinates (Gaia Collaboration 2018). We used both Topcat⁵ and Aladin⁶ Virtual Observatory tools with a small cross-match radius of 1.5 arcsec, and compared our results with those of Caballero (2017). Apart from the equatorial coordinates (Sect. 2.2.1), we also retrieved parallaxes, proper motions, radial velocities, and broadband magnitudes of the 165 stars and

³ <http://www.pa.uky.edu/~peter/newpage/>

⁴ <http://github.com/BU-hammerTeam/PyHammer>

⁵ <http://www.star.bris.ac.uk/~mbt/topcat/>

⁶ <http://aladin.u-strasbg.fr/AladinDesktop/>

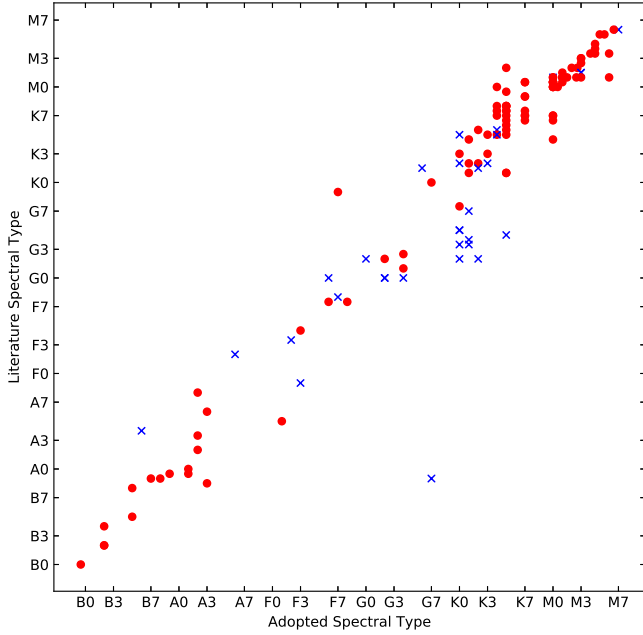


Fig. 1. Literature and adopted spectral types. Red filled circles and blue crosses stand for cluster members and non-members, respectively. Literature spectral types were retrieved from Greenstein & Keenan (1958), Guetter (1981), Nesterov et al. (1995), Wolk (1996), Houk & Swift (1999), Zapatero Osorio et al. (2002), Sacco et al. (2008), Caballero et al. (2008, 2012), Manara et al. (2013), and Hernández et al. (2014). The G7 star previously classified as A0 is “IDS 05335–0238 D”; the early spectral type may actually correspond to a close-by early A star at a few arcseconds (Hernández et al. 2014). The F7 star previously classified as K0 is Mayrit 968292; the late-G/early-K estimation from photometry by Caballero (2008a) was incorrect.

brown dwarfs. For the nine stars without *Gaia* DR2 parallaxes and proper motions, we took them from the existing literature (van Altena et al. 1995; Zacharias et al. 2005; van Leeuwen 2007; Altmann et al. 2017). Both proper motions and parallaxes are listed in Tables A.1 (IDS) and A.2 (OSIRIS), and are discussed in Sect. 3.1. The histograms of total proper motions and parallaxes for the complete sample are shown in Fig. 2. *Gaia* DR2 radial velocities are discussed in Sect. 3.3. Magnitudes will be presented in a forthcoming publication.

2.4. Youth features

We complemented our IDS, OSIRIS, and *Gaia* DR2 data with an exhaustive literature compilation of features of youth to support our determination of membership to the σ Orionis cluster. Below we describe each of the features that we looked for, together with EW(Li I) and EW(H α) from our spectra.

Lithium. Li I $\lambda 6707.80$ Å is the main indicator of youth in stars later than mid-F spectral type (Bertout 1989; Carlsson et al. 1994; Montes et al. 2001a; Zapatero Osorio et al. 2002). We highlight the fact that for open clusters as young as σ Orionis ($\tau \sim 3$ Ma) this is true only for low-mass stars with K and M spectral types, as Sun-like stars (spectral types F and G) do not have a deep convection zone and therefore lithium depletion occurs on longer time scales (Soderblom et al. 2014). We measured EW(Li I) in absorption in the IDS and OSIRIS spectra of 78 stars (Table A.5). Because of the low resolution of our spectra, especially for those obtained with OSIRIS and IDS R150V, we

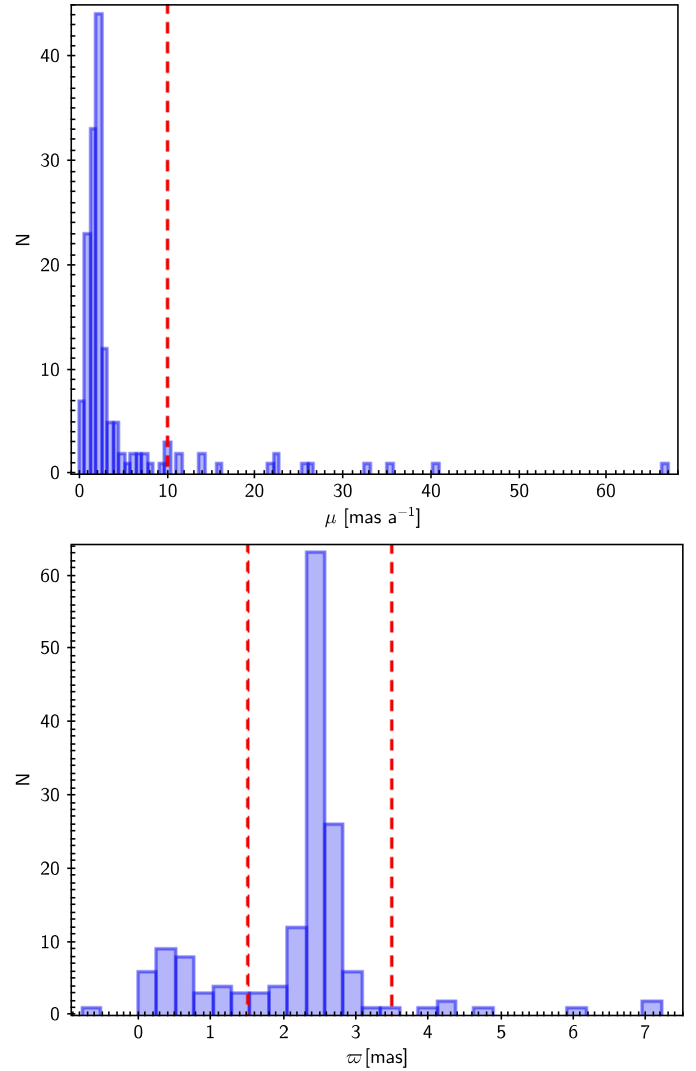


Fig. 2. Histograms of *Gaia* DR2 total proper motions (*top*) and parallaxes (*bottom*). Vertical dashed lines indicate the conservative σ Orionis boundary limits explained in Sect. 3.1. The bin sizes of these histograms have been adjusted according to Freedman & Diaconis (1981).

conservatively set a lower limit at $\text{EW}(\text{Li I}) = 0.1$ Å for claiming a true detection. We complemented our measurements with previous EW(Li I) values published by Zapatero Osorio et al. (2002), Kenyon et al. (2005), Sacco et al. (2008), and Hernández et al. (2014). Observations with higher spectral resolution and signal-to-noise ratio would be needed to disentangle the two populations of G- and K-type stars with very young ages in σ Orionis and with juvenile ages of up to 30 Ma in the cluster foreground.

Balmer series. In very young stars, H α $\lambda 6562.80$ Å can be in emission because of chromospheric emission or accretion from a circumstellar disc (Cram & Mullan 1979; Stauffer & Hartmann 1986; Bertout 1989; Barrado y Navascués & Martín 2003). We complemented our measurements with previous EW(H α) values or remarks published by Zapatero Osorio et al. (2002), Kenyon et al. (2005), Caballero (2008a), Sacco et al. (2008), and Hernández et al. (2014).

OB stars. Massive stars of early O and B spectral types stay in the main sequence for only a few million years. There are no evolved (i.e. giant) early-type stars in σ Orionis, providing

evidence for its extreme youth. Except for one anomalous example of a background B-type star, all O- and B-type stars in our sample, which were also the brightest targets that required the shortest exposure times, belong to the cluster (Caballero et al. 2007; Caballero 2008a – but see Sherry et al. 2008).

Mid-infrared. The flux excess in the mid-infrared (MIR) is produced by the presence of circum(sub)stellar discs around stars and brown dwarfs, and is often detected at the early stages of star formation (Muench et al. 2001; Lada et al. 2006; Fűrész et al. 2008). We searched for MIR indicators and Class I, II, and evolutionary and transition disc classification in Hernández et al. (2007), Luhman et al. (2008), and mostly compiled by Caballero (2008a).

X-rays. Although Garrison (1967) and Lyngå (1982) had already identified the star clustering, the importance of σ Orionis as a milestone star-forming region began with the discovery by Wolk (1996) of an agglomerate of intense X-ray-emitting stars densely concentrated around the eponymous σ Ori multiple star system. In general, the origin of X-ray emission lies on fast rotation and deep convective zones or wind collision (Pallavicini et al. 1981; Stelzer & Neuhäuser 2001; Favata & Micela 2003; Preibisch et al. 2005), depending on stellar mass. Here, we compiled X-ray detections from Franciosini et al. (2006), Skinner et al. (2008), López-Santiago & Caballero (2008), and Caballero et al. (2009, 2010).

Proper motion and parallax. Per se, proper motion (μ) and parallax (ϖ) are not youth features. However, all cluster members share common characteristics. In particular, they are located approximately in the same region of the sky and at the same distance, they move in the same direction with the same traverse velocity, have the same age and metallicity, and are born from the same parental cloud. Members within the μ and ϖ boundaries of the cluster are likely to have youth features. Vice versa, stars with μ and ϖ outside the cluster boundaries are likely to be devoid of youth features.

3. Results and discussion

3.1. Cluster membership

We used all available information to determine membership in σ Orionis of the 165 spectroscopically observed stars and brown dwarfs. We followed a step-by-step process, summarised in Table A.5:

– First, we discarded four T Tauri stars discovered by Haro & Moreno (1953) in neighbouring star-forming regions: Haro 5-17 in the eastern outskirts of the ϵ Orionis cluster (Collinder 1931; Caballero & Solano 2008), Haro 5-40 and Haro 5-44 near the Horsehead nebula (Pound et al. 2003; Habart et al. 2005; Goicoechea et al. 2006), and Haro 5-46 close to the Flame nebula (Mezger et al. 1988; Barnes et al. 1989; Bik et al. 2003). The four H α -emitter stars are located to the west of the Ori OB1b association, but at angular separations much greater than the extension of the halo of the σ Orionis cluster at 0.5 deg from the cluster centre, which is defined by the σ Ori Trapezium-like system (Caballero 2008b). The remaining 161 stars and brown dwarfs were located at less than 0.5 deg from the centre.

– We next applied the same astrometric criteria with *Gaia* DR2 data for cluster membership as in Caballero (2018), which represented an improvement with respect to those presented in Caballero (2010a). In particular, we discarded 51

stars with total proper motions $\mu > 10 \text{ mas a}^{-1}$ and/or parallaxes less than 1.5 mas or greater than 3.5 mas. The parallax criterion translated into discarding all stars with distances outside the 290–670 pc interval (assuming $d = 1/\varpi$; the precise σ Orionis distance of Schaefer et al. 2016 was 387.5 ± 1.3 pc). Careful inspection of the six *Gaia* DR2 sources with parallax uncertainties greater than 20% led to the recovery of Mayrit 1073209, an M3.0 star with youth features but with poor *Gaia* DR2 astrometric quality flags (astrometric_gof_al, astrometric_chi2_al, astrometric_excess_noise and, especially, the [re-normalised] unit-weight errors UWE and RUWE)⁷.

– Of the 110 remaining stars we identify OB spectral types in 11 cases, Li I in absorption in 87 (34 for the first time) cases, H α in emission in 67 (12 for the first time) cases, MIR excess in 46 cases, and X-ray emission in 63 cases. A few photometric cluster member candidates continue in the same state.

As expected, none of the astrometrically discarded stars displayed lithium in absorption, MIR excess, or X-ray emission. Many do not follow the spectro-photometric cluster sequence, either. However, there are two distant stars with faint and strong H α emission: IRAS 05358–0238 and StHa 50, respectively. The former is an evolved star at $d = 1.7^{+0.9}_{-0.5}$ kpc (Bailer-Jones et al. 2018) with a weak silicate feature and structure in the 10–12 μm range (Oliveira & van Loon 2004), while the later is an unusual, isolated Herbig Ae/Be star in the background at $d = 2.01^{+0.21}_{-0.18}$ kpc (Caballero 2017; Bailer-Jones et al. 2018). In spite of having been identified as a non-cluster-member over a decade ago (Caballero 2008a), IRAS 05358–0238 has since been observed with expensive facilities such as SCUBA and *Herschel* (Williams et al. 2013; Maucó et al. 2016).

Of the 51 foreground and background stars, 16 have previously been classified as such (e.g. Warren & Hesser 1977; Sherry et al. 2004; Caballero 2007). However, remarkably, 35 stars, which are listed in Table 3, were classified as cluster-member candidates in the extensive surveys of Hernández et al. (2007) and Caballero (2008a). Although additional cluster member candidates were discarded afterwards (e.g. in previous items of this series of papers or by Hernández et al. 2014), such a large number of new non-members has serious implications for a number of key science cases in the σ Orionis cluster. We qualitatively outline below some of the most relevant implications: (i) Hernández et al. (2007) determined frequencies of discs in a sample of 336 σ Orionis Herbig Ae/Be and T Tauri star candidates ranging from 10% to 35%, approximately, depending on stellar mass. A stellar population smaller by 10% may translate into an increase in the frequency of discs in intermediate-mass T Tauri stars to almost 40%; (ii) Peña Ramírez et al. (2012) determined the most comprehensive mass function (mass spectrum) of the cluster from about $20 M_{\odot}$ to about $0.005 M_{\odot}$ (see also Caballero 2011). These latter authors built this mass spectrum with the help of the Mayrit catalogue (Caballero 2008a) with the latest updates available that moment. The lack of 27 stars with estimated masses around $0.5 M_{\odot}$ can make a sharper contrast between the steep Salpeter’s region at more than $1 M_{\odot}$ and the almost flat slope of the mass spectrum at the lowest masses (Kroupa 2001; Chabrier 2003); (iii) Most of the discarded stars are located relatively far from the cluster centre⁸.

⁷ <https://www.cosmos.esa.int/web/gaia/dr2-known-issues>

⁸ The Mayrit number indicates the angular separation to and position angle from the cluster centre; e.g. Mayrit 1045067 is at $\rho \approx 1045$ arcsec and $\theta \approx 67$ deg from σ Ori AB.

Table 3. Previous cluster member candidates discarded in this work.

Name	Mayrit	[HHM2007]	Reason for discarding
HD 294276	...	20	No μ , no ϖ
2MASS J05372885–0255555	1650224	...	No ϖ , no Li
HD 294274	...	168	No μ
SO210868	958292	...	No ϖ
[HHM2007] 244	882239	244	No μ , no Li
2MASS J05375789–0259536	1596206	...	No ϖ
TYC 4771-720-1	...	289	No μ
[W96] 4771–0950	717307	...	No μ
[HHM2007] 385	733222	385	No μ , no ϖ , no Li
TYC 4771-873-1	1064335	...	No ϖ
[SE2004] 10	1564345	...	No ϖ , no Li
IRAS 05358–0238	377264	...	No ϖ , no Li
2MASS J05382265–0257421	1343194	...	No ϖ , no Li
StHa 50	459340	...	No ϖ
[W96] pJ053834–0239	258215	...	No ϖ , no Li
IDS 05335–0238 D	240322	...	No μ
[HHM2007] 648	...	648	No ϖ
[SE2004] 30	1045356	...	No ϖ , no Li
[W96] pJ053844–0233	123000	...	No ϖ , no Li
[HHM2007] 829	...	829	No μ , no ϖ
[HHM2007] 846	...	846	No ϖ , no Li
[HHM2007] 961	...	961	No μ , no ϖ
[SE2004] 50	945030	...	No ϖ , no Li
TYC 4771-661-1	...	1001	No μ , no ϖ
[HHM2007] 1009	735131	1009	No ϖ , no Li
[HHM2007] 1092	861056	1092	No ϖ , no Li
[HHM2007] 1129	1165138	1129	No ϖ , no Li
HD 294299	1037054	1163	No ϖ
[HHM2007] 1189	936072	1189	No ϖ , no Li
[HHM2007] 1251	1107114	1251	No ϖ , no Li
[HHM2007] 1256	1110113	1256	No ϖ
[HHM2007] 1269	1169117	1269	No ϖ , no Li
[HHM2007] 1347	1338116	1347	No ϖ , no Li
HD 294301	1468100	...	No μ
HD 294297	1659068	...	No μ , no ϖ

Notes. This table may be completed with Mayrit 1285339 (HD 294268, [HHM2017] 411) and Mayrit 1275190 based on discordant radial velocities (Sect. 3.3).

Therefore, while the cluster core may follow the same power law in the radial distribution presented by Caballero (2008b), the halo at angular separations $\rho \gtrsim 20$ arcsec could be even more rarefied. In other words, σ Orionis could be more compact than previously thought, which would ease the separation of its young population from other nearby young populations (Horsehead and Flame nebulae, ϵ Orionis); (iv) To date, the only metallicity determination based on a significantly large sample of stars in the cluster was performed by González Hernández et al. (2008). Looking back to their stellar sample with our current knowledge, the average cluster [Fe/H] value may be different from what they derived, albeit still near solar.

Regarding cluster members and member candidates in particular, while there are a few stars with the four youth features (Li I, H α , MIR, X-rays), apart from μ and d within the suitable intervals, there are also some member candidates that only follow the spectro-photometric sequence of the cluster. This is the case especially for relatively inactive A- and early-F-type stars, which have hot effective temperatures that prevent the formation of Li I and of deep convective zones (and, thus, strong magnetic fields) and, in addition, have short disc-dissipation

times. The list of photometric members without spectroscopic confirmation includes Mayrit 11238 (σ Ori C itself; A2 V). Besides, Mayrit 1227243 (HD 294275; A1 V) was classified by Caballero (2017) as a non-cluster-member based on a TGAS (Altmann et al. 2017) parallax that was quite different from the new *Gaia* DR2 one, which is compatible with cluster membership, and therefore it stands as a photometric member candidate.

In addition, we identified for the first time spectral features of youth (especially, but not only, Li I) in six stars that were previously photometric cluster-member candidates: Mayrit 144349, 1042077, 1082115, 1273081, and 1476077. We also assigned new Mayrit designations to two stars: Mayrit 1045067AB ([BMZ2001] S Ori J053948.1–022914; M3.0), for which lithium was not appreciable in our OSIRIS spectrum but for which low-gravity features were detected by Burningham et al. (2005), and Mayrit 1042077 ([HHM2007] 1250; K7), with a new Li I detection. Some faint targets with controversial detections of youth features, such as Mayrit 1298302 and Mayrit 1500066, require further investigation.

Figure 3 shows the measured EW(Li I) as a function of adopted spectral type. The earliest σ Orionis star for which

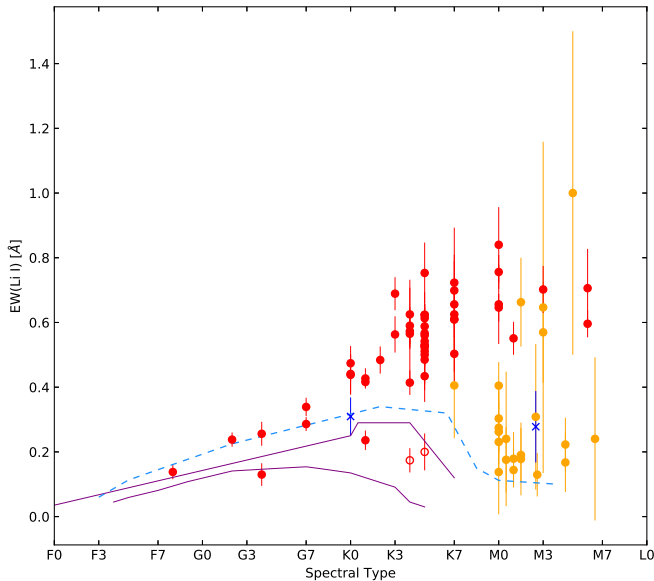


Fig. 3. Measured Li I EWs as a function of adopted spectral type. Filled red circles show young targets observed with IDS R1200Y; open red circles show young targets observed with IDS R150V (controversial); filled orange circles show young targets observed with OSIRIS R100B; blue crosses show non-member stars with Li I (Haro 5-17 and Haro 5-46); solid magenta lines show upper and lower EW(Li I) envelopes of the Pleiades ($\tau \sim 120$ Ma – Soderblom et al. 1993; Montes et al. 2001b); and the dashed cyan line shows the upper EW(Li I) envelope of IC 2602 ($\tau \sim 30$ Ma – Neuhauser et al. 1997).

we measured EW(Li I) is Mayrit 1285339 (HD 294268; F8 e). Pérez-Blanco et al. (2018) classified this object as a relatively evolved star in the sparse population of the Orion OB1 association. Our classification as a true cluster member is in accordance with the fact that the star hosts a transitional disc (Williams et al. 2013; Brown et al. 2013; Ansdell et al. 2017; Péricaud et al. 2017). However, since there are Herbig Ae/Be and classical T Tauri stars (with different kinds of discs) in the sparse population of the Orion OB1 association (e.g. Hernández et al. 2005; Briceño et al. 2019), there is still a possibility that Mayrit 1285339 actually belongs to that sparse population and not to the σ Orionis cluster. This argument is supported mainly by the radial velocity analysis of Pérez-Blanco et al. (2018). Mayrit 1285339 and some G- and K-type stars observed with IDS R1200Y and EW(Li I) within the envelopes of the Pleiades cluster are discussed in Sect. 3.3.

3.2. Strong accretors

The $H\alpha$ line is the atomic line for which we have the largest number of measurements, either in emission or in absorption. Figure 4 shows the distribution of our EW($H\alpha$) measurements. The vast majority of these lie in the interval from $+17 \text{ \AA}$ in absorption (for late B and early A stars) to -40 \AA in emission. However, there is a tail of very strong emitters, with EW($H\alpha$) down to -160 \AA , which correspond to objects that undergo accretion from a circum(sub)stellar disc. In particular, there are 40 σ Orionis stars and brown dwarfs in our sample that satisfy the Barrado y Navascués & Martín (2003) criterion for separating classical T Tauri objects with accretion from weak-line T Tauri objects with chromospheric activity. One non-cluster-member, the background Herbig Ae/Be star StHa 50, is above the coarse extrapolation of that criterion to spectral types earlier than K. The four discarded T Tauri stars discovered by Haro & Moreno (1953)

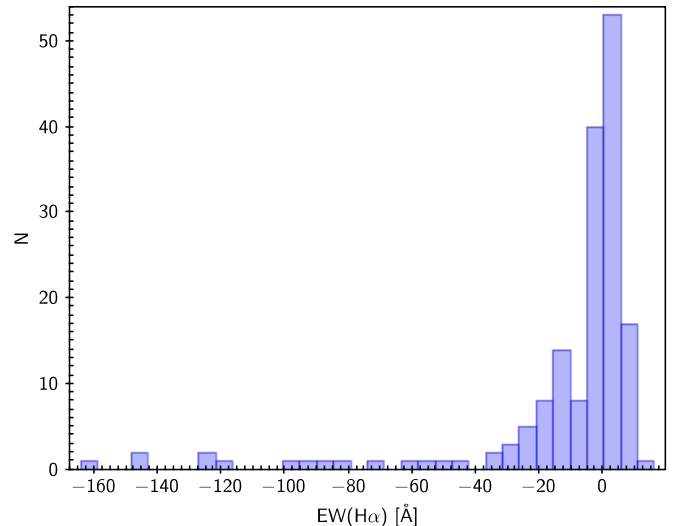


Fig. 4. Histogram of the number of sources as a function of the measured EW($H\alpha$). The bin size of this histogram has been adjusted according to Freedman & Diaconis (1981).

are also above the accretional/chromospheric activity boundary (Fig. 5).

Of the 40 accreting cluster members, 12 are young cluster members with EW($H\alpha$) $< -50 \text{ \AA}$, and are listed in Table 4, together with two Haro objects in IC 434. All of these 12 also have EW($H\beta$) $< -12 \text{ \AA}$ and significant emission in all observable Balmer lines, except for the M6.5-type brown dwarf Mayrit 1196092 ($J \approx 15.3$ mag), whose blue spectrum is too noisy. Table 4 includes: the brown dwarf mentioned immediately above; two objects at the stellar/substellar boundary at $J \approx 14.5$ mag (Caballero et al. 2007), namely Mayrit 1316178 and Mayrit 1364078, which also have M6.5 adopted spectral types; seven photometrically variable sources (Fedorovich 1960; Caballero et al. 2004); three stars with Li I in absorption detected for the first time; and three stars and one brown dwarf with EW($H\alpha$) measured for the first time (including the two Haro stars in IC 434).

After correcting heliocentric radial velocities using the IRAF `bcvcorr` task and smoothing the spectra with grade-two splines, we measured the shift of the centroid of the $H\alpha$ line (Fig. 6) and found five stars with displacements with respect to the air wavelength greater than 2.5 \AA , which translates into gas velocities greater than about 120 km s^{-1} . These five stars are ideal targets for searches for new faint jets in σ Orionis as discovered recently by Riaz et al. (2019).

Remarkably, nine of the 14 stars in Table 4 were discovered in objective-prism photographic plates by a small team of Mexican astronomers back in the middle of the twentieth century (Haro & Moreno 1953).

3.3. Binaries

On the one hand, in Fig. 3 there are two mid-type stars with relatively small EW(Li I) for their effective temperatures. These are Mayrit 863116 (HD 294300; G4) and Mayrit 1415279AB (OriNTT 429; K1). The latter is a spectroscopic binary discovered by Lee et al. (1994). As discussed in detail by Caballero (2010b)⁹, this double star shows a lower EW(Li I) than its actual

⁹ This is a summary in English of Caballero (2006, PhD Thesis, Universidad de La Laguna, Spain).

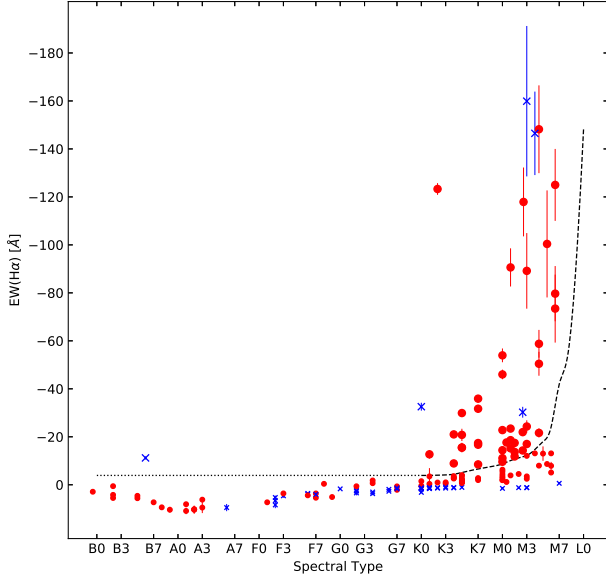


Fig. 5. Measured $EW(H\alpha)$ of our sample of stars as a function of adopted spectral type. The black dashed line shows the curve fitting from K0 to L0 of the EWs used in [Barrado y Navascués & Martín \(2003\)](#) as an empirical criterion for identifying classical T Tauri stars. The black dotted line shows the coarse extrapolation of the [Barrado y Navascués & Martín \(2003\)](#) criterion to spectral types earlier than K0 ($EW(H\alpha) = -3.9 \text{ \AA}$). Big and small red filled circles indicate cluster member stars and brown dwarfs with EWs above and below the black lines, respectively. Big and small blue crosses show non-cluster-member stars with EWs above and below the black lines, respectively. The early K-type σ Orionis star with strong emission is Mayrit 871071 (Haro 5-27, V510 Ori), the driving source of the jet HH 444 ([Reipurth et al. 1998](#); [López-Martín et al. 2001](#)).

value when observed in low spectral resolution (the combined spectrum of the red- and blueshifted components is smoothed by the low resolution).

On the other hand, there are another two classical T Tauri stars in [Fig. 3](#) with youth features and proper motions consistent with σ Orionis membership, but with abnormal *Gaia* DR2 parallaxes and low-quality astrometric flags. These are Mayrit 359179AB (V595 Ori) and Mayrit 873229AB (Haro 5-7), which were classified by [Caballero et al. \(2018\)](#) as a resolved binary and a binary candidate, respectively, with angular separations $\rho < 1$ arcsec (Mayrit 873229AB is also a double-line spectroscopic binary; [Maxted et al. 2008](#)).

Based on these two facts, close binarity could explain part of the scatter in the $EW(Li I)$ versus spectral-type diagram in [Fig. 3](#) (and in colour-magnitude diagrams), as well as inconsistencies between spectroscopic and astrometric data. Multiplicity in the σ Orionis cluster was reviewed in detail by [Caballero \(2014\)](#) and updated by [Caballero et al. \(2018\)](#). Following the procedure of the latter publication, we looked in *Gaia* DR2 for close binaries ($\rho < 4$ arcsec) among the investigated stars. Our results are summarised in [Table 5](#).

With the help of the Topcat Virtual Observatory tool, we identified and measured angular separation ρ , position angle θ , and magnitude difference in the *Gaia* broadband filter ΔG for 11 σ Orionis stars (at *Gaia* DR2 epoch J2015.5). We were also able to measure magnitude differences in the blue and red *Gaia* filters ΔB_p and ΔR_p for 5 of those 11. Of the 11 binaries, 6 had been discovered by [Caballero \(2008a, 2010a,b\)](#) and [Caballero et al. \(2018\)](#). Another two, indicated with parenthesis under “Reference” in [Table 5](#), were presented as binary candi-

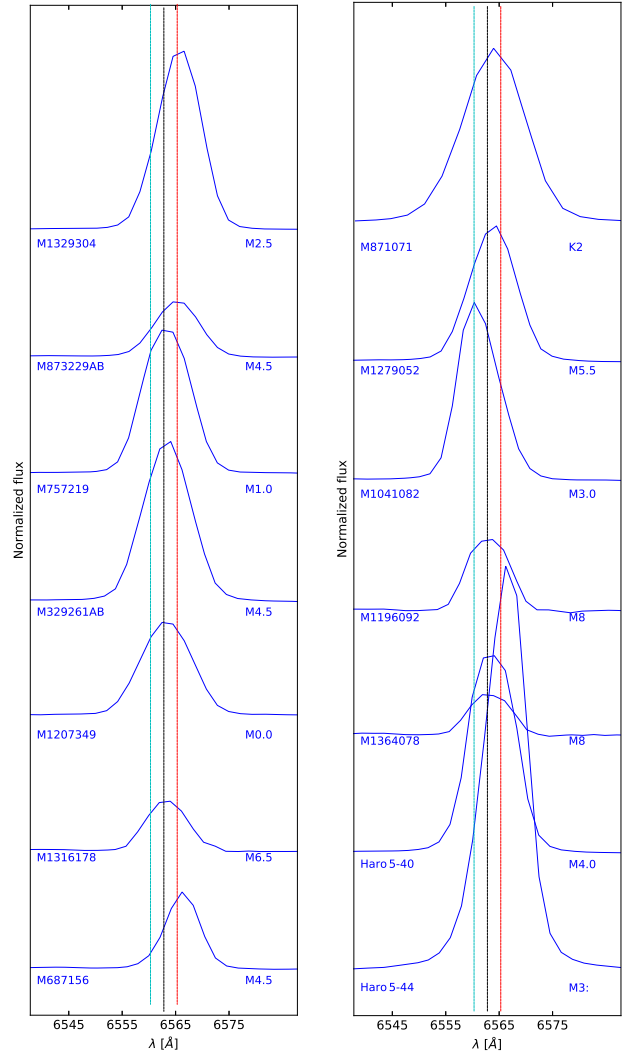


Fig. 6. Normalised spectra around $H\alpha \lambda 6562.80 \text{ \AA}$ of the 14 strong accretors in [Table 4](#). The vertical lines show the $H\alpha$ line shifted by -2.5 \AA (cyan), 0.0 \AA (black), and $+2.5 \text{ \AA}$ (red).

dates by [Caballero et al. \(2018\)](#), but these latter authors were only able to impose upper limits on angular separation. In summary, we discovered three new close binaries, namely Mayrit 329261AB, Mayrit 1045067AB, and Mayrit 1248183AB, and measured ρ and θ for the first time for another two close binaries, namely Mayrit 873229AB and Mayrit 1626148AB. Of these five objects, only the equal-mass Mayrit 1045067AB binary has an angular separation greater than 0.90 arcsec. The eponymous σ Ori multiple system, which contains at least five stars with spectral types between B2 V and O9.5 V ([Caballero 2014](#); [Simón-Díaz et al. 2015](#); [Maíz Apellániz et al. 2018](#), and references therein), is not resolved by *Gaia*.

As illustrated by [Fig. 7](#), we also retrieved *Gaia* DR2 radial velocities for 14 σ Orionis stellar members (and for 32 non-cluster-members), and found three young stars with radial velocities discordant with that of the cluster by more than 3σ : Mayrit 822170 ([W96] 4771–0119), Mayrit 1275190, and Mayrit 1285339 (HD 294268). The case of the T Tauri star Mayrit 822170 is striking, as it has lithium in absorption and $H\alpha$ and X-rays in emission but a radial velocity of $-32 \pm 6 \text{ km s}^{-1}$, vastly different from the $+31.10 \pm 0.16 \text{ km s}^{-1}$ determined by [Simón-Díaz et al. \(2015\)](#) for the open cluster. We looked for additional radial-velocity determinations on

Table 4. Strongly accreting stars and brown dwarfs with $EW(H\alpha) < -50 \text{ \AA}$.

Mayrit	Alternative name	H α emitter name	Variable name	SpT adopted	EW(H α) [\AA]	Remarks
Mayrit 1329304	Haro 5-5	Haro 5-5	...	M2.5	-118^{+14}_{-15}	EW(Li I) this work; red-shifted H α
Mayrit 873229AB	Haro 5-7	ESO-Ha 1646	NSV 2489	M4.5	-59^{+5}_{-6}	Red-shifted H α
Mayrit 757219	Haro 5-8	Kiso A-0976 322	SVS 1241	M1.0	-91^{+7}_{-9}	
Mayrit 329261AB	[SWW2004] 207	M4.5	-148^{+16}_{-20}	EW(H α) this work
Mayrit 1207349	Haro 5-9	Kiso A-0976 330	V2731 Ori	M0.0	-54^{+3}_{-3}	
Mayrit 1316178	S Ori J053847.2-025756	M6.5	-80^{+10}_{-13}	EW(H α) this work
Mayrit 687156	[WB2004] 26	ESO-Ha 1693	...	M4.5	-50^{+4}_{-6}	EW(Li I) this work; red-shifted H α
Mayrit 871071	Haro 5-27	Kiso A-0976 356	V510 Ori	K2	-123^{+2}_{-3}	Source of HH 444
Mayrit 1279052	Haro 5-30	Haro 5-30	...	M5.5	-100^{+20}_{-25}	
Mayrit 1041082	Haro 5-32	Kiso A-0976 359	V604 Ori	M3.0	-89^{+12}_{-19}	Blue-shifted H α
Mayrit 1196092	S Ori J054004.5-023642	M6.5	-125^{+15}_{-15}	EW(Li I) this work; brown dwarf
Mayrit 1364078	V2754 Ori	...	V2754 Ori	M6.5	-73^{+10}_{-19}	
...	Haro 5-40	Kiso A-0976 375	...	M4.0	-147^{+11}_{-21}	EW(H α) this work; IC 434
...	Haro 5-44	Kiso A-0904 111	V612 Ori	M3:	-160^{+28}_{-35}	EW(H α) this work; red-shifted H α ; IC 434

Table 5. Young binary stars in our sample resolved by *Gaia*.

Mayrit	ρ [arcsec]	θ [deg]	ΔB_p [mag]	ΔG [mag]	ΔR_p [mag]	Reference
873229AB	0.78	313.6	...	2.74	...	This work
329261AB	0.90	80.5	...	3.00	...	This work
168291AB	3.25	55.4	1.35	1.82	2.03	Cab10a
1248183AB	0.76	224.5	...	3.33	...	This work
359179AB	0.99	226.9	...	1.55	...	Cab18
707162AB	1.07	88.7	...	1.46	...	Cab10b
1626148AB	0.64	133.7	-0.07	0.15	-0.02	This work
960106AB	3.25	233.6	...	6.10	...	Cab18
1106058AB	2.68	219.5	3.75	3.88	3.15	Cab08
1045067AB	1.35	197.4	0.57	0.041	0.14	This work
1245057AB	2.14	4.3	0.31	0.0019	-0.11	Cab08

References. Cab08: Caballero (2008a); Cab10a: Caballero (2010a); Cab10b: Caballero (2010b); Cab18: Caballero et al. (2018).

these three stars in the studies by Jeffries et al. (2006), Caballero (2010b), Maxted et al. (2008), Sacco et al. (2008), Hernández et al. (2014), and Kounkel et al. (2018). Our findings are summarised in Table 6. The observed discordances are likely due to membership to the sparse foreground population of the Orion OB1 association (Mayrit 1275190 and, especially, Mayrit 1285339; Pérez-Blanco et al. 2018) or to the presence of an unseen companion (Mayrit 822170). The same may apply to the other young stars with low EW(Li I) for their spectral type or abnormal radial velocities and parallaxes. If both Mayrit 1275190 and Mayrit 1285339, at 21.3–21.4 arcmin to the cluster centre, actually belonged to a distinct population, the list of previous cluster member candidates discarded in this work (Table 3) would increase to 37 and in addition σ Orionis would be spatially more compact.

There are six tight binary systems among the 11 investigated *Gaia* DR2 sources with the highest RUWE values (Sect. 3.1):

σ Ori AB ($\rho \approx 0.266$ arcsec – Burnham 1892; Turner et al. 2008; Simón-Díaz et al. 2011), Mayrit 528005AB ([W96] 4771–899, $\rho \approx 0.40$ arcsec – Caballero 2005), and four of the five young binary stars in our sample resolved by *Gaia* (Table 5) with angular separations between 0.6 and 1.0 arcsec. All six have RUWE values greater than 3.8, much larger than the maximum value of 1.4 recommended for reliable astrometry by the *Gaia* Data Processing and Analysis Consortium (cf., Sect. 3.1). The fifth resolved binary, with $\rho \approx 0.90$ arcsec, $\Delta G \approx 3.00$ mag, and $RUWE \approx 1.23$, is Mayrit 329261AB ([SWW2004] 207), for which Sherry et al. (2004) reported a very nearby source with similar optical magnitudes ([SWW2004] 103). The other five stars sorted by RUWE values from 21.8 to 5.0 are Mayrit 203283, 1082115, 1073209, 521199, and 157155. All five of them have at least Li I in absorption and are thought to be single, with one of them, namely Mayrit 521199 (TX Ori), displaying all the attributes of a classical T Tauri star. Alternatively, these five objects could be

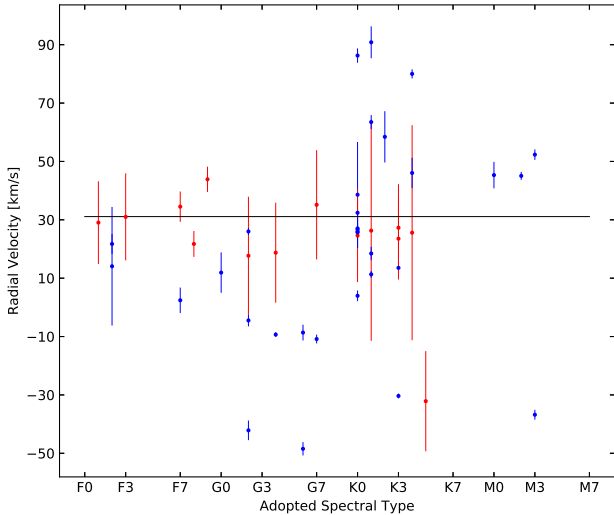


Fig. 7. *Gaia* DR2 radial velocity as a function of adopted spectral type. Red and blue circles highlight σ Orionis stars and non-cluster-member stars, respectively; coloured vertical error bars show 3σ uncertainties; and the black horizontal line shows the σ Ori systemic velocity $\gamma = +31.10 \pm 0.16 \text{ km s}^{-1}$.

tight binaries yet unresolved by *Gaia*, with angular separations of 0.5 arcsec or less.

4. Summary

We present a new detailed characterisation of 111 σ Orionis cluster members with spectral types from O9.5 to M6.5, 4 T Tauri stars in neighbouring star-forming regions, and 51 foreground and background stars. Our target sample includes OB stars in Trapezium-like systems, Herbig Ae/Be and T Tauri stars, and brown dwarfs with ages of about 3 Ma, in addition to peculiar interloper stars of different ages and evolutionary stages.

We used low-resolution optical spectroscopy collected with IDS at the INT and OSIRIS at the GTC to identify new youth features (mostly Li I in absorption and Balmer lines in emission) and to determine spectral types, *Gaia* DR2 proper motions, parallaxes, and photometry. We also used Virtual Observatory tools to astrometrically discard cluster members and to find close binaries, and literature information, such as X-ray emission, MIR flux excess, and previous measurements of Li I and $H\alpha$, for previous and relevant information. The combination of all these data allowed us to carry out an exhaustive membership classification and thereby form a more detailed picture of the σ Orionis stellar and substellar populations.

Perhaps the most remarkable result is the finding that 35 of those 51 non-cluster-member stars were previously classified and considered as cluster members in highly cited works on disc frequency and characterisation, initial mass function, spatial distribution, and chemical abundances. These 35 stars represent about 10% of the whole σ Orionis stellar population, and very likely a higher fraction at intermediate masses ($M \sim 0.5\text{--}1.0 M_{\odot}$), which has a significant impact on the results shown in previous works.

In addition, we have found: 14 strong accretors with $\text{EW}(\alpha) < -50 \text{ \AA}$, of which 2 are new identifications and 4 have measured $\text{EW}(H\alpha)$ for the first time; 5 strong accretors with significant blue- or redshift of the $H\alpha$ line, which can host undetected jets; 11 astrometric binaries with angular separations of 0.6–3.2 arcsec, of which 3 are discovered here and 5 have mea-

Table 6. Three Mayrit stars with discordant radial velocities.

Mayrit	V_r [km s^{-1}]		
	Her14	Kou18	<i>Gaia</i>
822170	$+34.0 \pm 0.8$	$+33.09 \pm 0.47$	-32.15 ± 5.72
1275190	...	$+45.81 \pm 0.75$	$+43.88 \pm 1.44$
1285339	$+22.2 \pm 1.1$	$+22.90 \pm 0.63$	$+21.73 \pm 1.48$

References. Her14: [Hernández et al. \(2014\)](#); Kou18: [Kounkel et al. \(2018\)](#); *Gaia*: [Gaia Collaboration \(2018\)](#).

sured ρ and θ for the first time; 2 juvenile star candidates in the sparse population of the Ori OB1b association; and one spectroscopic candidate based on *Gaia* DR2 radial velocities. Another five cluster members could be tight binaries based on large values of *Gaia* DR2 re-normalised unit-weight errors.

This fourth paper of the series “Stars and brown dwarfs in the σ Orionis cluster” is a follow-on of the comprehensive analysis of the very young open cluster with perhaps the best-studied stellar and substellar populations. It is also a preliminary step for the improvement in the determination of key parameters in star formation: metallicity, multiplicity, slope of the mass spectrum, disc and jet frequency, and spatial concentration across the huge mass interval from 20 to $0.005 M_{\odot}$.

Acknowledgements. We thank the anonymous referee for the careful review, J. Sanz-Forcada for helpful comments on X-rays, and R. Campillo for starting working on the data during his MSc thesis. This article is based on observations made in the Observatorios de Canarias del IAC with the Gran Telescopio Canarias and *Isaac Newton* Telescope of the *Isaac Newton* Group of Telescopes, both installed at the Spanish Observatorio del Roque de los Muchachos of the Instituto de Astrofísica de Canarias, in the island of La Palma, Spain, under programs INT15-07A, GTC55-12A, and GTC30-12B. This research made use of the SIMBAD, operated at Centre de Données astronomiques de Strasbourg, France, and NASA’s Astrophysics Data System. Financial support was provided by the Universidad Complutense de Madrid, the Comunidad Autónoma de Madrid, the Spanish Ministerio de Ciencia, Innovación y Universidades and the European FEDER/ERF funds under grants AYA2016-79425-C3-1/2-P and the Centre of Excellence “Severo Ochoa” and “María de Maeztu” awards to the Instituto de Astrofísica de Canarias (SEV-2015-0548) and Centro de Astrobiología (MDM-2017-0737).

References

Alonso-Floriano, F. J., Morales, J. C., Caballero, J. A., et al. 2015, *A&A*, **577**, A128
 Altmann, M., Roeser, S., Demleitner, M., Bastian, U., & Schilbach, E. 2017, *A&A*, **600**, L4
 Álvarez-Meraz, R., Nagel, E., Rendon, F., & Barragán, O. 2017, *Rev. Mex. Astron. Astrofis.*, **53**, 275
 Ansdell, M., Williams, J. P., Manara, C. F., et al. 2017, *AJ*, **153**, 240
 Bailer-Jones, C. A. L., Rybizki, J., Fouesneau, M., Mantelet, G., & Andrae, R. 2018, *AJ*, **156**, 58
 Barnes, P. J., Crutcher, R. M., Biegging, J. H., Storey, J. W. V., & Willner, S. P. 1989, *ApJ*, **342**, 883
 Barrado y Navascués, D., & Martín, E. L. 2003, *AJ*, **126**, 2997
 Béjar, V. J. S., Osorio, M. R. Z., & Rebolo, R. 1999, *ApJ*, **521**, 671
 Bertout, C. 1989, *ARA&A*, **27**, 351
 Bik, A., Lenorzer, A., Kaper, L., et al. 2003, *A&A*, **404**, 249
 Boesgaard, A. M., & Tripicco, M. J. 1986, *ApJ*, **302**, L49
 Bouvier, J., Barrado, D., Moraux, E., et al. 2018, *A&A*, **613**, A63
 Briceño, C., Calvet, N., Hernández, J., et al. 2019, *AJ*, **157**, 85
 Brown, J. M., Pontoppidan, K. M., van Dishoeck, E. F., et al. 2013, *ApJ*, **770**, 94
 Burnham, S. W. 1892, *Astron. Nachr.*, **130**, 257
 Burningham, B., Naylor, T., Littlefair, S. P., & Jeffries, R. D. 2005, *MNRAS*, **356**, 1583
 Caballero, J. A. 2005, *Astron. Nachr.*, **326**, 1007
 Caballero, J. A. 2007, *A&A*, **466**, 917
 Caballero, J. A. 2008a, *A&A*, **478**, 667
 Caballero, J. A. 2008b, *MNRAS*, **383**, 375

- Caballero, J. A. 2010a, *A&A*, 514, A18
- Caballero, J. A. 2010b, *Astrophys. Space Sci. Proc.*, 14, 79
- Caballero, J. A. 2011, *Stellar Clusters & Associations: A RIA Workshop on Gaia*, 108
- Caballero, J. A. 2014, *Observatory*, 134, 273
- Caballero, J. A. 2017, *Astron. Nachr.*, 338, 629
- Caballero, J. A. 2018, *Res. Notes Am. Astron. Soc.*, 2, 25
- Caballero, J. A., & Solano, E. 2008, *A&A*, 485, 931
- Caballero, J. A., Béjar, V. J. S., Rebolo, R., & Zapatero Osorio, M. R. 2004, *A&A*, 424, 857
- Caballero, J. A., Béjar, V. J. S., Rebolo, R., et al. 2007, *A&A*, 470, 903
- Caballero, J. A., Valdivielso, L., Martín, E. L., et al. 2008, *A&A*, 491, 515
- Caballero, J. A., López-Santiago, J., de Castro, E., & Cornide, M. 2009, *AJ*, 137, 5012
- Caballero, J. A., Albacete-Colombo, J. F., & López-Santiago, J. 2010, *A&A*, 521, A45
- Caballero, J. A., Cabrera-Lavers, A., García-Álvarez, D., & Pascual, S. 2012, *A&A*, 546, A59
- Caballero, J. A., Bouy, H., & Lillo-Box, J. 2016, *Observatory*, 136, 226
- Caballero, J. A., Novalbos, I., Tobar, T., & Miret, F. X. 2018, *Astron. Nachr.*, 339, 60
- Carlsson, M., Rutten, R. J., Bruls, J. H. M. J., & Shchukina, N. G. 1994, *A&A*, 288, 860
- Cepa, J. 2010, *Astrophys. Space Sci. Proc.*, 14, 15
- Cepa, J., Aguiar, M., Escalera, V. G., et al. 2000, in *Optical and IR Telescope Instrumentation and Detectors*, Proc. SPIE, 4008, 623
- Chabrier, G. 2003, *PASP*, 115, 763
- Chaffee, F. H., Carbon, D. F., & Strom, S. E. 1971, *ApJ*, 166, 593
- Cody, A. M., & Hillenbrand, L. A. 2014, *ApJ*, 796, 129
- Collinder, P. 1931, *Ann. Obs. Lund*, 2, B1
- Cottle, J. N., Covey, K. R., Suárez, G., et al. 2018, *ApJS*, 236, 27
- Covey, K. R., Ivezić, Ž., Schlegel, D., et al. 2007, *AJ*, 134, 2398
- Cox, A. N. 2001, *Allen's Astrophysical Quantities* (Berlin: Springer)
- Cram, L. E., & Mullan, D. J. 1979, *ApJ*, 234, 579
- Davison, C. L., White, R. J., Henry, T. J., et al. 2015, *AJ*, 149, 106
- Elliott, P., Scholz, A., Jayawardhana, R., Eisloffel, J., & Hébrard, E. M. 2017, *A&A*, 608, A66
- Falcón-Barroso, J., Sánchez-Blázquez, P., Vazdekis, A., et al. 2011, *A&A*, 532, A95
- Favata, F., & Micela, G. 2003, *Sci. Space Rev.*, 108, 577
- Fedorovich, V. P. 1960, *Perem. Zvezdy*, 13, 166
- Fűrész, G., Hartmann, L. W., Megeath, S. T., Szentgyorgyi, A. H., & Hamden, E. T. 2008, *ApJ*, 676, 1109
- Franciosini, E., Pallavicini, R., & Sanz-Forcada, J. 2006, *A&A*, 446, 501
- Freedman, D., & Diaconis, P. 1981, *Zeitschrift für Wahrscheinlichkeitstheorie und Verwandte Gebiete*, 57, 453
- Gaia Collaboration (Prusti, T., et al.) 2016, *A&A*, 595, A1
- Gaia Collaboration (Brown, A. G. A., et al.) 2018, *A&A*, 616, A1
- Garrison, R. F. 1967, *PASP*, 79, 433
- Goicoechea, J. R., Pety, J., Gerin, M., et al. 2006, *A&A*, 456, 565
- González Hernández, J. I., Caballero, J. A., Rebolo, R., et al. 2008, *A&A*, 490, 1135
- Greenstein, J. L., & Keenan, P. C. 1958, *ApJ*, 127, 172
- Guetter, H. H. 1981, *AJ*, 86, 1057
- Habart, E., Abergel, A., Walmsley, C. M., Teyssier, D., & Pety, J. 2005, *A&A*, 437, 177
- Haro, G., & Moreno, A. 1953, *Boletín de los Observatorios Tonantzintla y Tacubaya*, 1, 11
- Herbig, G. H. 1962, *ApJ*, 135, 736
- Hernández, J., Calvet, N., Hartmann, L., et al. 2005, *AJ*, 129, 856
- Hernández, J., Hartmann, L., Megeath, T., et al. 2007, *ApJ*, 662, 1067
- Hernández, J., Calvet, N., Perez, A., et al. 2014, *ApJ*, 794, 36
- Houk, N., & Swift, C. 1999, *Michigan Catalogue of Two-dimensional Spectral Types for the HD Stars* (University of Michigan), 5
- Jeffries, R. D., Maxted, P. F. L., Oliveira, J. M., & Naylor, T. 2006, *MNRAS*, 371, L6
- Johnson, H. L., & Mitchell, R. I. 1958, *ApJ*, 128, 31
- Kenyon, M. J., Jeffries, R. D., Naylor, T., Oliveira, J. M., & Maxted, P. F. L. 2005, *MNRAS*, 356, 89
- Kirkpatrick, J. D., Henry, T. J., & McCarthy, Jr., D. W. 1991, *ApJS*, 77, 417
- Koenig, X., Hillenbrand, L. A., Padgett, D. L., & DeFelippis, D. 2015, *AJ*, 150, 100
- Kounkel, M., Covey, K., Suárez, G., et al. 2018, *AJ*, 156, 84
- Kroupa, P. 2001, *MNRAS*, 322, 231
- Lada, C. J., Muench, A. A., Luhman, K. L., et al. 2006, *AJ*, 131, 1574
- Lee, C. W., Martin, E. L., & Mathieu, R. D. 1994, *AJ*, 108, 1445
- Lépine, S., Hilton, E. J., Mann, A. W., et al. 2013, *AJ*, 145, 102
- López-Martín, L., Raga, A. C., López, J. A., & Meaburn, J. 2001, *A&A*, 371, 1118
- López-Santiago, J., & Caballero, J. A. 2008, *A&A*, 491, 961
- Luhman, K. L., Hernández, J., Downes, J. J., Hartmann, L., & Briceño, C. 2008, *ApJ*, 688, 362
- Lyngå, G. 1982, *A&A*, 109, 213
- Maíz Apellániz, J., Barbá, R. H., Simón-Díaz, S., et al. 2018, *A&A*, 615, A161
- Manara, C. F., Testi, L., Rigliaco, E., et al. 2013, *A&A*, 551, A107
- Martín, E. L., Lodieu, N., Pavlenko, Y., & Béjar, V. J. S. 2018, *ApJ*, 856, 40
- Maucó, K., Hernández, J., Calvet, N., et al. 2016, *ApJ*, 829, 38
- Maxted, P. F. L., Jeffries, R. D., Oliveira, J. M., Naylor, T., & Jackson, R. J. 2008, *MNRAS*, 385, 2210
- Metodieva, Y., Antonova, A., Golev, V., et al. 2015, *MNRAS*, 446, 3878
- Mezger, P. G., Chini, R., Kreysa, E., Wink, J. E., & Salter, C. J. 1988, *A&A*, 191, 44
- Montes, D., López-Santiago, J., Gálvez, M. C., et al. 2001a, *MNRAS*, 328, 45
- Montes, D., López-Santiago, J., Fernández-Figueroa, M. J., & Gálvez, M. C. 2001b, *A&A*, 379, 976
- Muench, A. A., Alves, J., Lada, C. J., & Lada, E. A. 2001, *ApJ*, 558, L51
- Nesterov, V. V., Kuzmin, A. V., Ashimbaeva, N. T., et al. 1995, *A&AS*, 110, 367
- Neuhäuser, R., Torres, G., Sterzik, M. F., & Randich, S. 1997, *A&A*, 325, 647
- Newton, E. R., Charbonneau, D., Irwin, J., et al. 2014, *AJ*, 147, 20
- Oliveira, J. M., & van Loon, J. T. 2004, *A&A*, 418, 663
- Pallavicini, R., Golub, L., Rosner, R., et al. 1981, *ApJ*, 248, 279
- Pecaut, M. J., & Mamajek, E. E. 2013, *ApJS*, 208, 9
- Peña Ramírez, K., Béjar, V. J. S., Zapatero Osorio, M. R., Petr-Gotzens, M. G., & Martín, E. L. 2012, *ApJ*, 754, 30
- Pérez-Blanco, A., Maucó, K., Hernández, J., et al. 2018, *ApJ*, 867, 116
- Péridaud, J., Di Folco, E., Dutrey, A., Guilloteau, S., & Piétu, V. 2017, *A&A*, 600, A62
- Perryman, M. A. C., Brown, A. G. A., Lebreton, Y., et al. 1998, *A&A*, 331, 81
- Popper, D. M. 1980, *ARA&A*, 18, 115
- Pound, M. W., Reipurth, B., & Bally, J. 2003, *AJ*, 125, 2108
- Preibisch, T., Kim, Y.-C., Favata, F., et al. 2005, *ApJS*, 160, 401
- Reipurth, B., Bally, J., Fesen, R. A., & Devine, D. 1998, *Nature*, 396, 343
- Ríaz, B., Gizis, J. E., & Harvin, J. 2006, *AJ*, 132, 866
- Ríaz, B., Briceño, C., Whelan, E. T., & Heathcote, S. 2017, *ApJ*, 844, 47
- Ríaz, B., Machida, M. N., & Stamatellos, D. 2019, *MNRAS*, 486, 4114
- Sacco, G. G., Randich, S., Franciosini, E., Pallavicini, R., & Palla, F. 2007, *A&A*, 462, L23
- Sacco, G. G., Franciosini, E., Randich, S., & Pallavicini, R. 2008, *A&A*, 488, 167
- Sánchez-Blázquez, P., Peletier, R. F., Jiménez-Vicente, J., et al. 2006, *MNRAS*, 371, 703
- Schaefer, G. H., Hummel, C. A., Gies, D. R., et al. 2016, *AJ*, 152, 213
- Sherry, W. H., Walter, F. M., & Wolk, S. J. 2004, *AJ*, 128, 2316
- Sherry, W. H., Walter, F. M., Wolk, S. J., & Adams, N. R. 2008, *AJ*, 135, 1616
- Simón-Díaz, S., Caballero, J. A., & Lorenzo, J. 2011, *ApJ*, 742, 55
- Simón-Díaz, S., Caballero, J. A., Lorenzo, J., et al. 2015, *ApJ*, 799, 169
- Skinner, S. L., Sokal, K. R., Cohen, D. H., et al. 2008, *ApJ*, 683, 796
- Skrutskie, M. F., Cutri, R. M., Stiening, R., et al. 2006, *AJ*, 131, 1163
- Soderblom, D. R., Jones, B. F., Balachandran, S., et al. 1993, *AJ*, 106, 1059
- Soderblom, D. R., Hillenbrand, L. A., Jeffries, R. D., Mamajek, E. E., & Naylor, T. 2014, in *Protostars and Planets VI*, eds. H. Beuther, R. S. Klessen, C. P. Dullemond, & T. Henning, 219
- Stauffer, J. R., & Hartmann, L. W. 1986, *ApJS*, 61, 531
- Stauffer, J. R., Schultz, G., & Kirkpatrick, J. D. 1998, *ApJ*, 499, L199
- Stelzer, B., & Neuhäuser, R. 2001, *A&A*, 377, 538
- Turner, N. H., ten Brummelaar, T. A., Roberts, L. C., et al. 2008, *AJ*, 136, 554
- van Altena, W. F., Lee, J. T., & Hoffleit, E. D. 1995, *The General Catalogue of Trigonometric Stellar Parallaxes* (New Haven, CT: Yale University Observatory)
- Vandenberg, D. A., & Bridges, T. J. 1984, *ApJ*, 278, 679
- van Leeuwen, F. 2007, *A&A*, 474, 653
- Vazdekis, A., Sánchez-Blázquez, P., Falcón-Barroso, J., et al. 2010, *MNRAS*, 404, 1639
- Walter, F. M., Sherry, W. H., Wolk, S. J., & Adams, N. R. 2008, *Handbook of Star Forming Regions*, 4, 732
- Warren, W. H., & Hesser, J. E. 1977, *ApJS*, 34, 115
- Williams, J. P., Cieza, L. A., Andrews, S. M., et al. 2013, *MNRAS*, 435, 1671
- Winter, A. J., Clarke, C. J., Rosotti, G., et al. 2018, *MNRAS*, 478, 2700
- Wolk, S. J. 1996, PhD Thesis, Harvard-Smithsonian Center for Astrophysics Cambridge, Massachusetts, USA
- Zacharias, N., Monet, D. G., Levine, S. E., et al. 2005, *VizieR Online Data Catalog: I/297*
- Zapatero Osorio, M. R., Béjar, V. J. S., Martín, E. L., et al. 2000, *Science*, 290, 103
- Zapatero Osorio, M. R., Béjar, V. J. S., Pavlenko, Y., et al. 2002, *A&A*, 384, 937
- Zapatero Osorio, M. R., Béjar, V. J. S., & Peña Ramírez, K. 2017, *ApJ*, 842, 65

Appendix A: Large-format figures and long tables

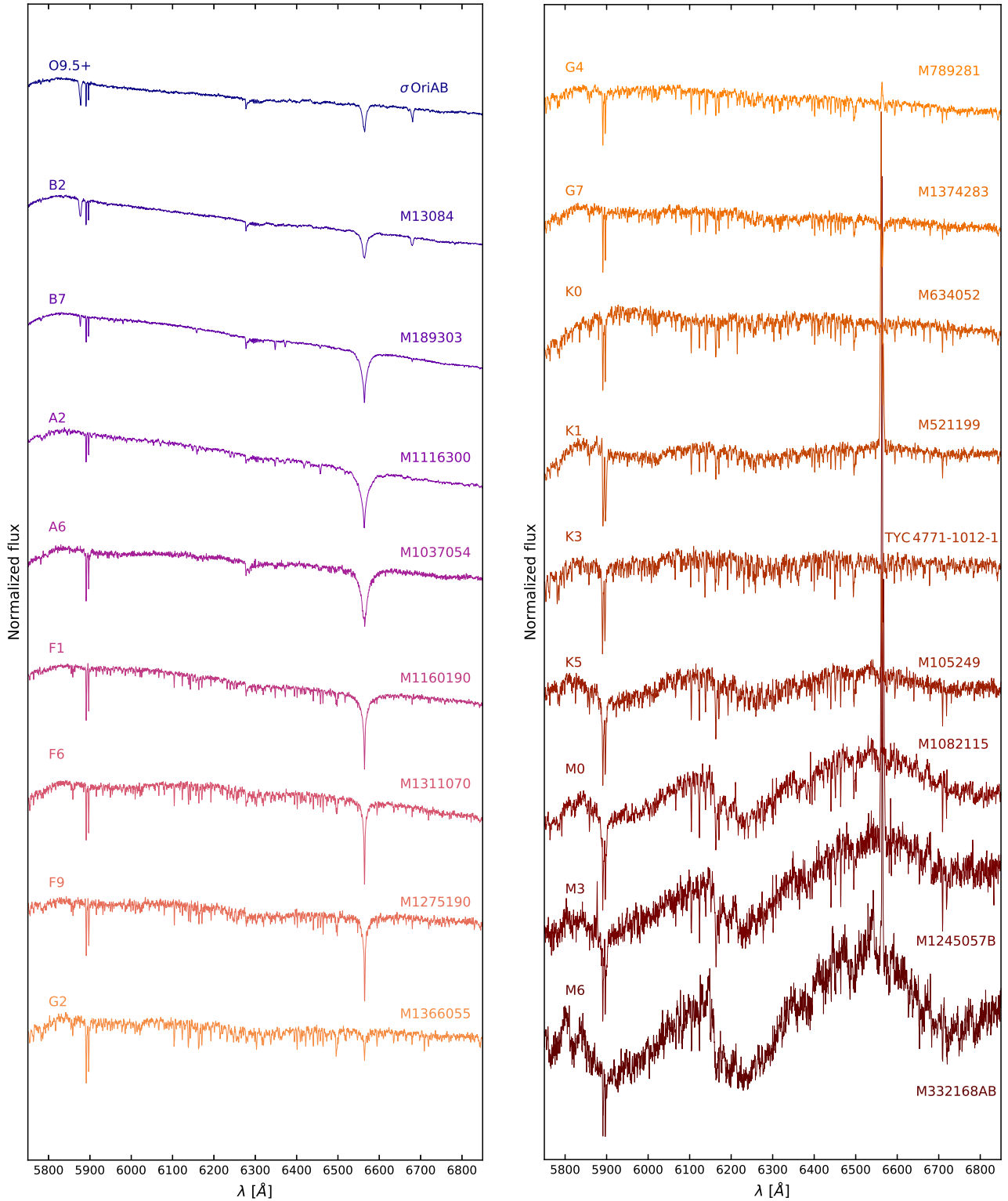


Fig. A.1. R1200Y IDS/INT spectra of 18 stars (most from σ Orionis) with spectral types from O9.5+ V to M6 in the wavelength range used for spectral-type identification.

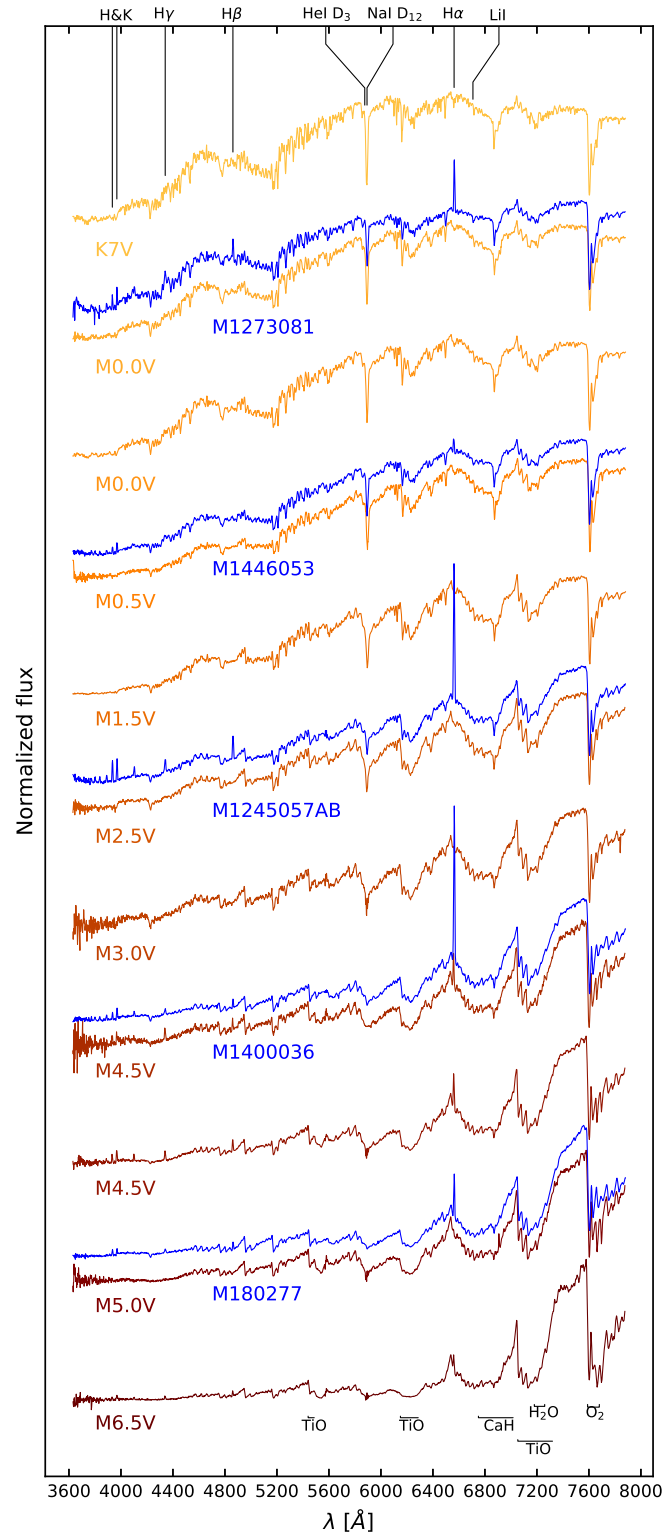


Fig. A.2. OSIRIS/GTC normalised spectra of five of the σ Orionis stars of different spectral types (in blue) on a grid of spectra of standard stars used for visual spectral-type identification of the OSIRIS spectra. The main spectral lines and most relevant absorption bands are also marked.

Table A.1. Observations of targets towards σ Orionis with IDS/INT.

Mayrit	Alternative name	α (J2000)	δ (J2000)	$\mu_\alpha \cos \delta$ [mas a ⁻¹]	μ_δ [mas a ⁻¹]	ϖ [mas]	Date of observation	t_{exp} [s]
...	TYC 4770-1018-1	05 36 57.15	-02 25 39.9	0.910 ± 0.086	-0.437 ± 0.080	0.554 ± 0.045	23 Feb. 2007	180
1456284	TYC 4770-1261-1	05 37 10.49	-02 30 07.1	0.748 ± 0.083	-9.226 ± 0.078	3.491 ± 0.040	23 Feb. 2007	240
							27 Feb. 2007	450
1415279AB	OriNTT 429	05 37 11.62	-02 32 08.8	0.639 ± 0.064	-0.773 ± 0.065	2.725 ± 0.036	24 Feb. 2007	300
							27 Feb. 2007	360
1374283	SO211394	05 37 15.37	-02 30 53.4	-0.341 ± 0.092	-1.029 ± 0.091	2.351 ± 0.048	23 Feb. 2007	300
...	HD 294270	05 37 18.82	-02 31 36.4	16.324 ± 0.096	-28.327 ± 0.094	2.808 ± 0.042	24 Feb. 2007	120
...	HD 294276	05 37 20.68	-02 49 33.1	6.823 ± 0.058	-65.963 ± 0.062	7.160 ± 0.039	22 Feb. 2007	120
(1650224)	2M J05372885-0255555	05 37 28.85	-02 55 55.6	0.207 ± 0.055	1.337 ± 0.058	0.485 ± 0.035	23 Feb. 2007	180
...	TYC 4770-1468-1	05 37 29.88	-02 43 45.7	-2.705 ± 0.065	-4.911 ± 0.063	0.709 ± 0.038	23 Feb. 2007	180
1227243	HD 294275	05 37 31.87	-02 45 18.5	-2.188 ± 0.084	-3.126 ± 0.085	2.849 ± 0.052	24 Feb. 2007	120

Notes. ^(a)2MASS J05381494-0219532 and 2MASS J05384652-0235479 had poor quality spectra and, therefore, were discarded from the analysis. ^(b)Mayrit 1500066 was not tabulated by *Gaia* DR2 and its equatorial coordinates are from 2MASS. ^(c)We took three spectra of Mayrit 1245057AB: one of component A, one of component B, and of the two of them inside the slit in parallactic angle. ^(d)Proper motions from Zacharias et al. (2005) (UCAC4). ^(e)Proper motions from Altmann et al. (2017) (HSOY). ^(f)We took two spectra of Mayrit 1626148AB: one of component A and one of component B. The full table is available at the CDS.

Table A.2. Observations of targets towards σ Orionis with OSIRIS/GTC.

Mayrit	Alternative name	α (J2000)	δ (J2000)	$\mu_\alpha \cos \delta$ [mas a ⁻¹]	μ_δ [mas a ⁻¹]	ϖ [mas]	Date of observation	t_{exp} [s]
1329304	Haro 5-5	05 37 30.95	-02 23 42.8	1.765 ± 0.082	-1.16 ± 0.079	2.731 ± 0.041	13 Nov. 2012	2 × 200
1298302 ^(d) ^(e)	[SWW2004] 137	05 37 31.54	-02 24 27.0	-3.393 ± 2.085	-1.398 ± 2.115	...	04 Mar. 2012	1 × 600
1129222	[WB2004] 10	05 37 53.98	-02 49 54.5	1.77 ± 0.25	-1.41 ± 0.21	2.53 ± 0.13	27 Dec. 2012	2 × 250
783254	2E 1455	05 37 54.40	-02 39 29.8	1.64 ± 0.12	-0.42 ± 0.10	2.590 ± 0.064	04 Mar. 2012	3 × 30
...	2E 1456	05 37 56.31	-02 45 13.2	0.8 ± 1.0	1.1 ± 1.1	-0.67 ± 0.59	17 Mar. 2012	1 × 1200
873229AB	Haro 5-7	05 38 01.08	-02 45 38.0	1.73 ± 0.57	-0.94 ± 0.52	4.23 ± 0.40	13 Nov. 2012	2 × 200
662301	Kiso A-0904 67	05 38 06.75	-02 30 22.7	1.035 ± 0.074	-0.383 ± 0.074	2.354 ± 0.042	04 Mar. 2012	2 × 300
1073209	[SWW2004] 52	05 38 09.95	-02 51 37.8	-0.23 ± 0.86	-0.08 ± 0.75	-0.73 ± 0.51	22 Dec. 2012	4 × 150
757219	Haro 5-8	05 38 13.15	-02 45 51.1	1.199 ± 0.072	-1.175 ± 0.065	2.518 ± 0.044	15 Nov. 2012	2 × 300
329261AB	[SWW2004] 207	05 38 23.08	-02 36 49.4	1.42 ± 0.25	-1.88 ± 0.21	1.92 ± 0.16	26 Dec. 2012	2 × 250

Notes. ^(a)The full alternative names of Mayrit 1316178, 897077, 1045067, and 1196092 are preceded by [BMZ2001]. ^(b)Mayrit 180277 was also observed on 06 Mar. 2012 at an airmass of 1.25 for 900 s with the volume-phase holographic grating R2500V ($R \sim 1400$, $\Delta\lambda \sim 4400-6000 \text{ \AA}$). ^(c)2E 1456 is a galaxy previously thought to be a star. We did not account for it in the analysis. ^(d)Mayrit 1298302 was not tabulated by *Gaia* DR2 and its equatorial coordinates are from 2MASS. ^(e)Proper motions from Altmann et al. (2017) (HSOY). ^(f)Proper motions from Zacharias et al. (2005) (UCAC4). The full table is available at the CDS.

Table A.3. Equivalent widths of IDS/INT spectra of stars and brown dwarfs towards σ Orionis.

Name	EW(H β) [\AA]	EW(He I D ₃) [\AA]	EW(H α) [\AA]	EW(Li I) [\AA]	SpT MILES	SpT PyHammer
TYC 4770-1018-1	+1.4 ^{+0.2} _{-0.3}	...	K0:	K0
Mayrit 1456284	+3.6 ^{+0.3} _{-0.3}	...	F7	G0
Mayrit 1415279AB	-0.37 ^{+0.10} _{-0.07}	+0.24 ^{+0.04} _{-0.02}	K1	K5
Mayrit 1374283	+2.1 ^{+0.4} _{-0.2}	+0.29 ^{+0.03} _{-0.02}	G7	K3
HD 294270	+3.6 ^{+0.5} _{-0.4}	...	F6:	F6
HD 294276	+3.0 ^{+0.5} _{-0.3}	...	G4	K0
2M J05372885-0255555	+1.8 ^{+0.2} _{-0.2}	...	K0	K3
TYC 4770-1468-1	+1.4 ^{+0.1} _{-0.2}	...	K1	K5
Mayrit 1227243	+11 ⁺¹ ₋₁	...	A1	A3
Mayrit 1116300	+10 ⁺² ₋₁	...	A2	A3

Notes. ^(a)Stars observed also with the R150V grism. The full table is available at the CDS.

Table A.4. Equivalent widths of OSIRIS/GTC spectra of stars and brown dwarfs towards σ Orionis.

Name	EW(Ca K) [Å]	EW(Ca H) [Å]	EW(H γ) [Å]	EW(H β) [Å]	EW(He I D ₃) [Å]	EW(H α) [Å]	EW(Li I) [Å]	SpT Standards	SpT PyHammer
Mayrit 1329304	-73^{+8}_{-12}	-57^{+7}_{-9}	-26^{+4}_{-5}	-56^{+5}_{-6}	$-3.3^{+0.3}_{-0.4}$	-118^{+14}_{-15}	$+0.13^{+0.06}_{-0.08}$	M2.5	M7
Mayrit 1298302 ^(a)	>-2.0	>-2.0	>-1.0	-2.6 ± 0.2	...	-3.5 ± 0.3	$<+0.2$	M3.0	M3
Mayrit 1129222	...	-25^{+7}_{-13}	-14^{+3}_{-3}	-12^{+2}_{-2}	$-1.4^{+0.3}_{-0.3}$	-22^{+1}_{-2}	$+0.31^{+0.18}_{-0.27}$	M2.5:	M6
Mayrit 783254 ^(a)	$+13 \pm 2$	$+9 \pm 2$	$+0.7 \pm 0.2$	$+0.8 \pm 0.6$...	$+0.8 \pm 0.2$	$+0.34 \pm 0.09$	$\ll K7$	K2
Mayrit 873229AB	-13^{+4}_{-5}	-25^{+4}_{-4}	-18^{+2}_{-3}	-19^{+2}_{-2}	$-2.3^{+0.5}_{-0.5}$	-59^{+5}_{-6}	...	M4.5	M7
Mayrit 662301 ^(a)	-5.5 ± 1.5	-5.5 ± 1.0	-9 ± 2	-7.0 ± 1.0	...	-11.8 ± 0.9	$+0.66 \pm 0.14$	M1.5	M1
Mayrit 1073209	-18^{+7}_{-4}	-15^{+4}_{-5}	$-9.2^{+2.2}_{-2.9}$	$-9.2^{+1.2}_{-2.3}$	$-1.2^{+0.3}_{-0.3}$	-24^{+2}_{-3}	$+0.57^{+0.11}_{-0.21}$	M3.0	M4
Mayrit 757219	-94^{+15}_{-21}	-74^{+11}_{-11}	-33^{+3}_{-5}	-49^{+5}_{-5}	$-2.2^{+0.3}_{-0.3}$	-91^{+7}_{-9}	$+0.14^{+0.05}_{-0.06}$	M1.0	M7
Mayrit 329261AB	-18^{+5}_{-9}	-29^{+5}_{-8}	-17^{+3}_{-5}	-52^{+10}_{-13}	$-5.7^{+0.8}_{-1.3}$	-148^{+16}_{-20}	...	M4.5	M8
Mayrit 609206 ^(a)	-26 ± 3	-26 ± 3	-9 ± 2	-15.0 ± 1.0	...	-46 ± 2	$+0.40 \pm 0.07$	M0:	M4

Notes. ^(a)Sources observed by Caballero et al. (2012). The full table is available at the CDS.

Table A.5. Membership and youth features of investigated stars ^(a).

Name	SpT Literature	Ref.	SpT Adopted	OB	μ	ϖ	Li I	H α	mIR	X rays	Member
TYC 4770-1018-1	K0:	○	×	×					×
Mayrit 1456284	F7	○	○				○		★
Mayrit 1415279AB	K2.0 \pm 1.0	Her14	K1	●	●	○			○		★
Mayrit 1374283	G7	●	●	○			○		★
HD 294270	G0	Nes95	F6:	×	●						×
HD 294276	G0	Nes95	G4	×	×						×
2M J05372885-0255555	K0	●	×	×					×
TYC 4770-1468-1	K1	○	×	×					×
Mayrit 1329304	M2.0 \pm 0.5	Her14	M2.5	●	●	●	○	○			★
Mayrit 1298302	M3.0 \pm 0.5	Cab12	M3.0						○		★

Notes. ^(a)Symbols: filled circles: for μ and ϖ , stars inside the cluster member boundaries, and for Li I and H α , stars for which we measured such lines for the first time; open circles: stars with previous measurements from the literature; filled stars: σ Orions members in this work; crosses: for μ and ϖ , stars outside the cluster member boundaries, for Li I, K and M stars for which we have not found Li I in absorption, and for the last column, fore- or background stars. ^(b)Parallax affected by close binarity. ^(c)Discordance in radial velocity. The full table is available at the CDS.

References. GK58: Greenstein & Keenan (1958); Gue81: Guetter (1981); Nes95: Nesterov et al. (1995); Wol96: Wolk (1996); HS99: Houk & Swift (1999); ZO02: Zapatero Osorio et al. (2002); Sac08: Sacco et al. (2008); Cab08: Caballero et al. (2008); Cab12: Caballero et al. (2012); Man13: Manara et al. (2013); Her14: Hernández et al. (2014).